Available online at www.sciencedirect.com
SCIENCE DIRECT®
Journal of Nuclear Materials 329–333 (2004) 304–308
journal of nuclear materials
www.elsevier.com/locate/jnucmat

Microstructural examination of low activation ferritic steels following irradiation in ORR at 330 and 400 °C to ~10 dpa

D.S. Gelles *

Pacific Northwest National Laboratory, P8-15, P.O. Box 999, Richland, WA 99352, USA [1]

Abstract

Microstructural examinations are reported for a series of low activation steels containing Mn following irradiation in the Oak Ridge Reactor at 330 and 400 °C to ~10 dpa. Alloy compositions included 2% Cr, 9% Cr and 12% Cr steels with V to 1.5% and W to 1.0%. Results include compositional changes in precipitates and microstructural changes as a function of composition and irradiation temperature. It is concluded that temperatures in ORR are on the order of 50 °C higher than anticipated.

1. Introduction

The post-irradiation tensile test response has been reported for a series of reduced activation alloys containing manganese following irradiation in the Oak Ridge Reactor (ORR) at 60, 200, 330, and 400 °C to ~10 dpa, [1] and shear punch behavior was reported for irradiated TEM disks that were irradiated under effectively identical conditions [2]. The alloys include 2% Cr alloys with V additions, and 9% and 12% Cr alloys containing Mn with V and W additions (Table 1). These alloys have been studied extensively prior to and following irradiation in the Fast Flux Test Facility in order to understand microstructural evolution in low activation alloys to high dose [3–6]. An alloy design concept involved substitution of Mn for Ni in order to control austenite stability. Unfortunately, subsequent experiments demonstrated that Mn additions resulted in unexpected Chi-phase precipitation. However, as Mn is formed by transmutation from Fe in a fusion environment, studies of effects of Mn on irradiation response in low activation alloys is pertinent. Recent improvements in specimen preparation technique now allow preparation of electron transparent foils from 1 mm diameter disks created during shear punch testing [7]. Smaller samples reduce magnetic and radioactivity effects allowing, for example, more effective determination of precipitate compositions. Therefore, this report is intended to describe microstructural examinations of the shear punch specimens, in order to provide understanding of the effects of irradiation on strength at temperatures below 400 °C.

2. Experimental procedure

Compositions and material identification codes for specimens irradiated in the ORR-MFE 6J and 7J tests are provided in Table 1. Specimens were of standard TEM geometry, 3 mm in diameter × 0.20 mm (reduced to 1 mm for examination.) The 6J test accumulated damage levels of 6.6–6.8 dpa and the 7J test accumulated 7.1–7.3 dpa, variations corresponding to lower or higher chromium levels [8,9]. Predicted helium levels are 2.1–2.3 appm for both tests, with variations due to higher or lower chromium levels, respectively. Specimens in 6J, designed to operate at 330 °C, included the two digit location code LB, and specimens in 7J, designed to operate at 400 °C, included the two digit location code

* Tel.: +1-509 376 3141; +1-509 376 0418.
E-mail address: ds_gelles@pnl.gov (D.S. Gelles).
[1] Pacific Northwest National Laboratory (PNNL) is operated by the U.S. Department of Energy by Battelle Memorial Institute under contract DE-AC06-76RLO-1830.

0022-3115/$ - see front matter © 2004 Elsevier B.V. All rights reserved.
doi:10.1016/j.jnucmat.2004.04.049

Table 1
Identification codes and compositions for TEM specimens irradiated in the ORR-MFE 6J and 7J tests [1]

ID code	Composition (w/o)					
	Cr	V	W	Mo	C	Mn
P3	2.25	0.5			0.1	
P4	2.25	1.0			0.1	
P5	2.25	1.5		0.2	0.1	0.3
RB	9	0.3	1.0		0.1	2.5
P6	9	0.5			0.1	
P9	9	0.5			0.1	2.0
P7	9	1.3			0.2	1.0
RE	12	0.3	1.0		0.1	6.5
RA	12	1.0			0.1	6.5

LH, so that each specimen for examination is identified with a unique four digit code defining both material and irradiation conditions.

Examinations were performed on a JEOL 1200EX for microstructural features and on a JEOL 2010F for precipitate composition information. Precipitate particles were chosen for analysis close to the edge of the foil in order to minimize compositional effects from the surrounding matrix. Measurements employed Oxford Instruments ISIS software in STEM mode. A typical run involved capturing an image, selecting points for analysis including nearby matrix and hole count for each image and storing the acquired spectra for later analysis. It should be noted that despite the shift to 1 mm samples, effects of magnetism and background radioactivity remained. The background subtraction was performed in order to obtain a level for Mn comparable to the starting composition, assuming in effect, that Mn did not segregate to precipitates. However, the most useful parameters defining carbide compositions are considered to be the V/Cr and W/Cr ratios.

3. Results

The results of this study will be divided into four sections. First, microstructural results for low Cr, intermediate Cr and higher Cr alloys will be presented successively and then results of precipitate compositional analysis will be provided.

3.1. Low Cr

The 2% Cr alloys were found to contain both a fine dislocation structure and fine precipitates following irradiation at 330 °C. Following irradiation at 400 °C, the structures were similar but on a coarser scale. No void swelling was found following irradiation at either temperature. Examples of the microstructures are shown in Figs. 1–3. For each specimen, a series of two micro-

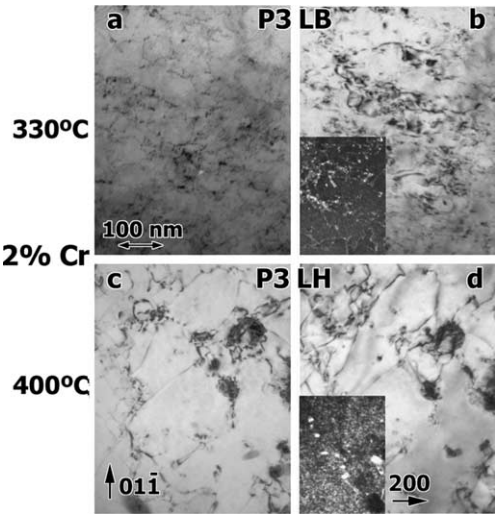

Fig. 1. Microstructures in 2Cr–0.5V.

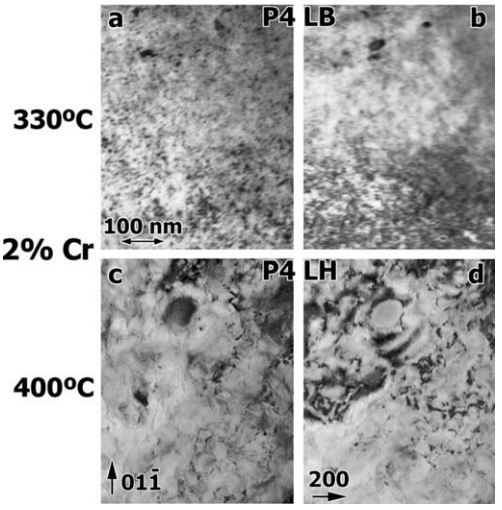

Fig. 2. Microstructures in 2Cr–1V.

graphs is provided, generally taken of the same area near an (0 1 1) orientation, the one on the left using $\bar{g} = 0\,1\,\bar{1}$ with $\bar{g}$ vertical, and the one on the right using $\bar{g} = 2\,0\,0$ with $\bar{g}$ horizontal. This configuration allows straightforward differentiation of $a\langle 1\,0\,0\rangle$ Burgers vectors that should appear as strong vertical images in 200 contrast. For example, from Fig. 1, it can be concluded that most of the dislocations are probably of $\frac{a}{2}\langle 1\,1\,1\rangle$ character. Fig. 1 contains insets using 200 dark field contrast in order to emphasize that the smaller features have quite different contrast from the dislocation structure, indicating the presence of precipitates as small as 4 nm following irradiation at 330 °C and ~8 nm at 400 °C. Similar structure on a denser scale is found with increasing V

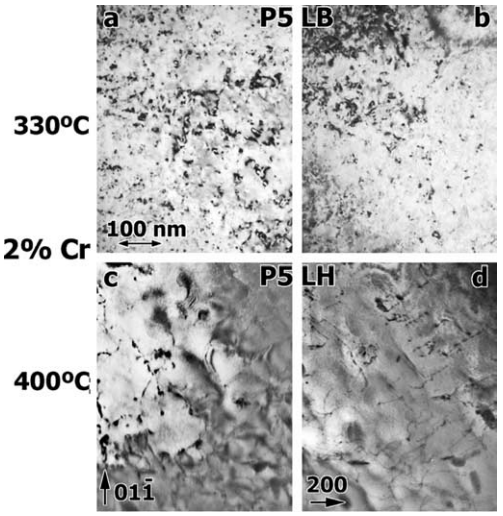

Fig. 3. Microstructures in 2Cr–1.5V–0.3Mn–0.2Mo.

content. (Note that images for specimen P4LB show a thicker area.) In specimen P4LH, it was possible to demonstrate that the fine precipitate often appears as square platelets on (1 0 0) planes. Therefore, precipitates appear to increase in number density with increasing V content.

3.2. Intermediate Cr

Alloys containing 9% Cr also were generally found to contain both a fine dislocation structure and fine precipitates following irradiation at 330 °C. Behavior observed in condition P9LB was atypical in that the dislocation structure was found to be quite coarse. This may indicate additions of Mn may discourage precipitation when V levels are low. The structures following irradiation at 400 °C showed little evidence of precipitation apart from the large carbides probably remaining from preirradiation heat treatment. Again, no void swelling was found following irradiation at either temperature. Examples are provided in Figs. 4–6. In all cases, an example following irradiation at 330 °C is given but only two examples of behavior at 400 °C are included. Note that the orientation for Fig. 6 is close to (0 0 1).

3.3. Higher Cr

The 12% Cr alloys were found to respond to irradiation somewhat differently than the low and intermediate Cr alloys. The difference in dislocation density was smaller as a function of irradiation temperature (lower at low temperatures and higher at higher temperatures than for lower Cr alloys), and extensive precipitation was found following irradiation at 400 °C. However, again no void swelling was observed. Examples are provided in Figs. 7 and 8. The precipitation found following irradiation at 400 °C can be seen in Figs. 7(d) and 8(d) (provided at higher magnification) and is typical of α', the Cr-rich bcc phase.

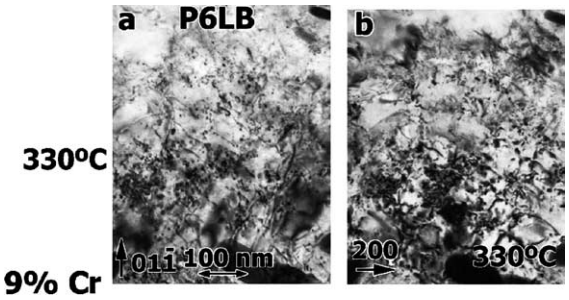

Fig. 4. Microstructures in 9Cr–0.5V.

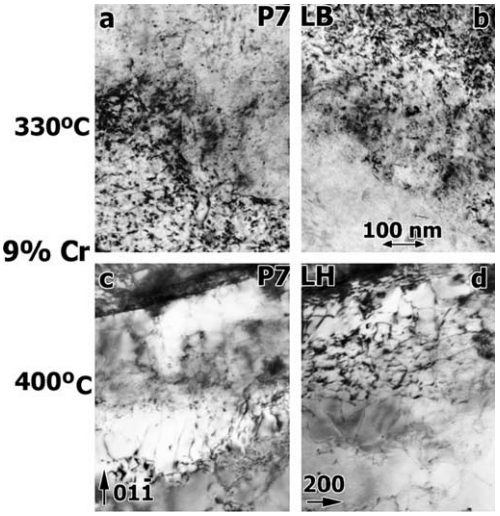

Fig. 5. Microstructures in 9Cr–1.3V–1Mn.

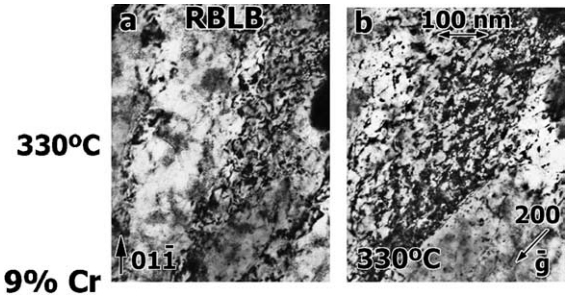

Fig. 6. Microstructures in 9Cr–1W–0.3V–2.5Mn.

3.4. Precipitate compositions

Compositions for precipitate particles in foils of each specimen were measured on at least 20 particles near or overhanging foil edges. This included both irradiation

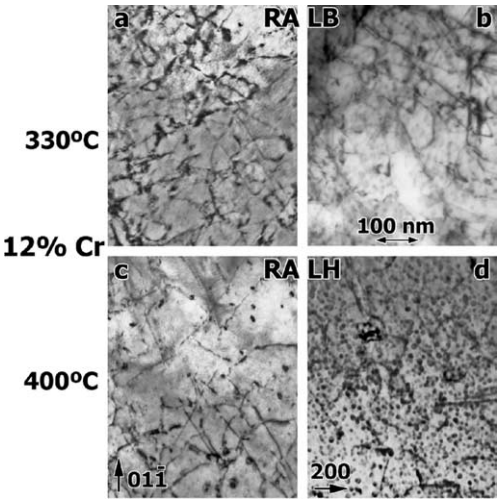

Fig. 7. Microstructures in 12Cr–1V–6.5Mn.

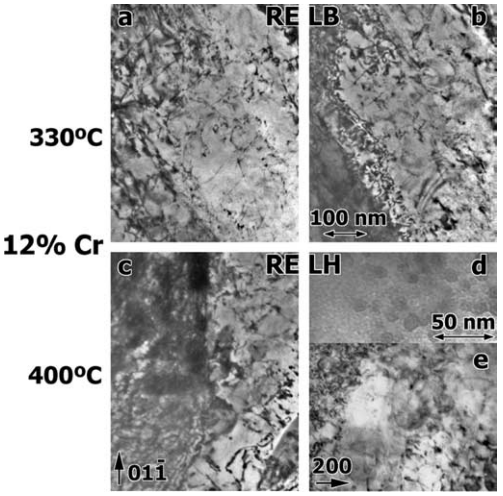

Fig. 8. Microstructures in 12Cr–1W–0.3V–6.5Mn.

conditions, irradiated at 330 and 400 °C, and results are provided in Table 2. The compilation in Table 2 tends to emphasize maximum observed levels of V and Cr (and therefore lowest levels of Fe), ignoring determinations where levels were lower, on the assumption that higher levels of Fe corresponded to inclusion of matrix information. However, the V/Cr and W/Cr ratios reported include particles with higher levels of Fe.

Of particular note are inclusion of results for α' in RALH and a phase with high Fe noted for P4LB. Compositional measurements of α' demonstrate high levels of Cr, as anticipated. Such measurements are rare. These measurements were made in TEM mode for particles that happened to hang over the edge of the foil, apparently because the electropolishing conditions left them unaffected. An example of similar microstructure found in condition RELH is inset in Fig. 8(d). Also of note is that the phase in P4LB with high Fe cannot be heavily matrix-contaminated MC because Cr levels are too high but it does not match the phase called M_7C_3. Although, the identity of this phase is not yet apparent, it provides an explanation for behavior, as will be discussed.

4. Discussion

The results of this investigation follow previously observed trends from this alloy series [3–6]. Identical specimens have been previously studied following irradiation in the Fast Flux Test Facility (FFTF) at 420 °C to doses from 7.7 to 200 dpa. In general, fine precipitation was found in the 2% Cr alloys following irradiation, assumed to be of MC (V_4C_3) type. Also, evidence for α' was apparent in 12% Cr alloy microstructures. Precipitate compositions were provided for extracted precipitates following irradiation at 520 °C to 14.5 dpa that are in agreement with the present results except that M_7C_3 was not found in 2Cr alloys (due to the higher temperature) and W levels were higher in alloys containing W following irradiation at 520 °C.

However, significant differences can be identified. As noted, no voids were observed following irradiation in ORR whereas a few voids were identified in FFTF irradiated Fe–9Cr–1V–1Mn (corresponding to condition P7) after 7.7 dpa at 420 °C. Also, dislocation structures appeared different, with more $a\langle 1\,0\,0\rangle$ Burgers vectors evident in FFTF irradiated specimens. Finally, α' precipitation in 12% Cr alloys was finer following irradiation in FFTF (~10 nm) than in ORR (~20 nm). As temperature control was believed to be more accurate in FFTF than in ORR (as it was based on direct reading thermocouples in contact with sodium coolant), it is anticipated that the irradiation temperature in the ORR 7J test is closer to 450 °C. This temperature difference along with effects of flux variation can be expected to explain unexpected swelling and dislocation differences between FFTF and ORR. The temperature of the ORR 6J capsule is expected to be significantly below 420 °C because the 6J microstructures are much finer than those from FFTF irradiation at 420 °C, but no comparable irradiation tests are available to determine if it also ran hotter than expected.

An objective of this work was to compare microstructural observations with mechanical properties response for identical conditions. A compilation of the mechanical properties can be found in reference [2]. As to be expected, higher irradiation temperatures produced coarser microstructures and lower strengths. Differences were not as great for 12% Cr alloys, explainable based on the distribution of α' and its effect on dislocation density. The α' precipitation formed after irradiation of 12% Cr alloys at 400 °C, whereas other

Table 2
Precipitate compositions in wt% (excluding measurements designated as matrix)

Code	Metal composition	Fe	Cr	Mn	V	W	V/Cr:W/Cr	Ident.
P3LB	Fe–2.25Cr–0.5V	47–50	42–45	0	3.6–8.1	–	0.07–0.18	M_7C_3
P3LB	Fe–2.25Cr–0.5V	12–21	10–11	0	68–78	–	6–7.9	MC
P3LH	Fe–2.25Cr–0.5V	46–50	45–51	0.3	3.2–5.7	–	0.06– 0.13	M_7C_3
P3LH	Fe–2.25Cr–0.5V	45–49	6–12	0.3	50–80	–	5.3–8.7	MC
P4LB	Fe–2.25Cr–1V	85–90	5.7–11	0	3.5–4.9	–	0.4–1.2	MC
P4LB	Fe–2.25Cr–1V	12–36	4.5–18	0	51–81	–	7–14	?
P4LH	Fe–2.25Cr–1V	12–29	25–41	0	35–41	–	0.8–1.8	MC
P5LB	Fe–2.25Cr–1.5V–0.3Mn–0.2Mo	73–94	3.0–6.9	0.3	2.5–20	–	1.5–2.5	M_7C_3
P5LB	Fe–2.25Cr–1.5V–0.3Mn–0.2Mo	7–30	4.8–5.1	0.3	65–87	–	13–16	MC
P5LH	Fe–2.25Cr–1.5V–0.3Mn–0.2Mo	20–26	65–71	0.3	8.4–10	–	0.12–0.15	M_7C_3?
P6LB	Fe–9Cr–0.5V	22–35	57–67	0	7.3–11	–	0.11–0.17	$M_{23}C_6$
P9LB	Fe–9Cr–0.5V–2Mn	na	na	na	na	–	na	na
P9LH	Fe–9Cr–0.5V–2Mn	19–34	59–74	2.0	4.7–5	–	0.06–0.09	$M_{23}C_6$
P7LB	Fe–9Cr–1.3V–1Mn	20–34	62–72	1.0	2.5–7.8	–	0.06–0.16	$M_{23}C_6$
P7LB	Fe–9Cr–1.3V–1Mn	15	15	1.0	69	–	4.2	MC
P7LH	Fe–9Cr–1.3V–1Mn	18–29	61–69	1.0	7.8–11	–	0.13–0.17	$M_{23}C_6$
RALB	Fe–12Cr–1V–6.5Mn	28–64	39–62	6.5	1.7–5.7	–	0.08–0.13	$M_{23}Ce$
RALH	Fe–12Cr–1V–6.5Mn	5–31	60–94	6.5	1.2–3.8	–	0.02–0.04	σ'
RALH	Fe–12Cr–1V–6.5Mn	24	65	6.5	4.7	–		$M_{23}C_6$
RBLB	Fe–9Cr–1W–0.3V–2.5Mn	28–34	49–57	6.5	1.1–1.5	7.5–10	0.02:0.12	$M_{23}C_6$
RBLB	Fe–9Cr–1W–0.3V–2.5Mn	41	45	6.5	5.3	2.6	0.11:0.06	σ?
RBLH								
RELB	Fe–12Cr–1W–0.3V–6.5Mn	19–42	46–70	6.5	0.8–2.9	1.5–9.8	0.04:0.1	$M_{23}C_6$
RELH	Fe–12Cr–1W–0.3V–6.5Mn	23–29	59–61	6.5	6.0–9.9	0.2–0.9	0.15:0.01	$M_{23}C_6$

alloys only showed coarse carbide structures following irradiation at the higher temperature. The 9% Cr alloys contained the simplest microstructures and showed the weakest behavior. However, the behavior for 2% Cr alloys was more complex. The microstructural trends in the 2% Cr alloys showed increasing precipitation with increasing V. However, the mechanical properties showed maximum strength at 0.5 V, minimum hardening at 1.0 V and intermediate hardening (but failure before yielding in tensile testing) at 1.5 V. Therefore, microstructural studies do not directly explain behavior. Perhaps an explanation lies in the observation of somewhat different precipitates in P4, i.e. the unidentified phase with higher Fe concentrations. Alternatively, more detailed examinations may be required to find structure on a finer scale, such as was done for F82H to explain hardening at low temperatures [10].

5. Conclusions

A series of low activation alloys that were irradiated as TEM disks in the ORR have been examined by TEM following shear punch testing. Small 1 mm specimen geometries simplified microstructural examinations and compositional analyses but did not eliminate problems. In general, observed behavior reflected previous observations of these alloys following irradiation in FFTF. However, dislocation structures differed due to more coarse structure and less $a\langle 1\,0\,0\rangle$ development, no void swelling was found, and α' was coarser. In part, these differences are ascribed to higher than expected temperatures in the 7J test.

References

[1] M.L. Hamilton, D.S. Gelles, J. Nucl. Mater. 307–311 (2002) 256.
[2] R.M. Ermi, M.L. Hamilton, D.S. Gelles and A.M. Ermi, DOE/ER-0313/29 (2000) 103.
[3] D.S. Gelles and M.L. Hamilton, DOE/ER-0045/13 (1985) 128.
[4] D.S. Gelles and M.L. Hamilton, DOE/ER-0045/16 (1986) 131.
[5] D.S. Gelles, in: R.L. Klueh, D.S. Gelles, M. Okada, N.H. Packan, (Eds.), Reduced Activation Materials for Fusion Reactors ASTM STP 1047, ASTM, Philadelphia, PA, 1990, p. 113.
[6] D.S. Gelles, DOE/ER-0313/15 (1994) 156.
[7] S. Ohnuki, K. Shiba, Y. Kohno, A. Kohyama, J.P. Robertson, M.L. Hamilton, D.S. Gelles, MRS Symposium Proceedings 540 (1999) 603.
[8] L.R. Greenwood, DOE/ER-0313/6 (1989) 23.
[9] L.R. Greenwood, DOE/ER-0313/8 (1990) 34.
[10] R. Schaeublin, D.S. Gelles, M. Victoria, J. Nucl. Mater. 307–311 (2002) 197.